

Article

# CATS: Context-Aware Traffic Signal Control with Road Navigation Service for Connected and Automated Vehicles

Yiwen Shen 

The Department of Software and Computer Engineering, Ajou University, Suwon 16499, Republic of Korea; chrisshen@ajou.ac.kr

## Abstract

Urban intersection traffic signals play a crucial role in managing traffic flow and ensuring road safety. However, traditional actuated signal controllers make phase-switching decisions based on limited local traffic information, without leveraging network-wide context from navigation services. In this paper, we propose CATS, a Context-Aware Traffic Signal control system that jointly optimizes intersection signal control and road navigation for Connected and Automated Vehicles (CAVs). CATS integrates two key components: a Best-Combination CTR (BC-CTR) scheme and the Self-Adaptive Interactive Navigation Tool (SAINT). BC-CTR enhances the original Cumulative Travel-Time Responsive (CTR) scheme through a two-step selection procedure: it first identifies the phase with the highest cumulative travel time (CTT) and then selects the compatible phase combination with the greatest group CTT, providing an explicit improvement over the single-combination evaluation of the original CTR that allows for a more accurate response to real-time intersection demand. SAINT provides congestion-aware route guidance via a congestion-contribution step function, directing vehicles away from congested segments while signal timings simultaneously adapt to incoming traffic. Under a 100% CAV penetration setting, SUMO-based simulations across moderate-to-heavy traffic conditions (vehicle inter-arrival times of 5 to 9 s) show that CATS reduces the mean end-to-end travel time by up to 23.72% and improves the throughput by up to 93.19% over three baselines (fixed-time navigation with enhanced signal control, congestion-aware navigation with original signal control, and fixed-time navigation with original signal control), confirming that the co-design of navigation and signal control produces complementary benefits.

**Keywords:** context-aware traffic signal control; connected and automated vehicles; road navigation service; cumulative travel-time responsive; actuated traffic signal; urban traffic management



Academic Editor: Yung-Fa Huang

Received: 30 March 2026

Revised: 12 April 2026

Accepted: 17 April 2026

Published: 20 April 2026

**Copyright:** © 2026 by the author.

Licensee MDPI, Basel, Switzerland.

This article is an open access article

distributed under the terms and

conditions of the [Creative Commons](https://creativecommons.org/licenses/by/4.0/)

[Attribution \(CC BY\)](https://creativecommons.org/licenses/by/4.0/) license.

## 1. Introduction

Urban traffic congestion imposes substantial economic, environmental, and safety costs on modern cities, with inefficient intersection management being one of its primary drivers [1]. Traffic signals, if well-coordinated, have the potential to reduce vehicle waiting times, increase road throughput, and lower fuel consumption and emissions (or battery power consumption) across an entire road network. Connected and Automated Vehicles (CAVs) further amplify this opportunity: by sharing real-time position, speed, and routing data with roadside infrastructure, CAVs enable signal controllers and navigation services to access network-wide traffic information that was previously unavailable to fixed or isolated

systems [2,3]. Realizing this potential, however, requires a tighter integration between traffic signal control and route guidance than what current systems provide.

Existing actuated signal control methods, such as the Cumulative Travel-Time Responsive (CTR) scheme [4], improve upon fixed-time plans by dynamically adjusting phase durations based on real-time vehicle demand at individual intersections. However, these methods suffer from two fundamental limitations. First, they make phase-selection decisions using only local, intersection-level information, without exploiting the network-wide context available from navigation services. In particular, the original CTR selects the next phase based solely on the single phase combination with the largest group cumulative travel time (CTT), which can overlook higher-demand compatible phase combinations at the same intersection. Second, route guidance systems such as shortest-path Dijkstra navigation operate independently of the traffic signal state, and thus, vehicles are distributed across the road network without regard to how their routing decisions will affect signal queues or downstream congestion patterns. This decoupling means that navigation may channel vehicles onto routes that create avoidable signal bottlenecks, while signal controllers simultaneously operate without awareness of incoming vehicle load predicted by the navigation service. As a result, neither component alone can achieve the system-level efficiency that the tight co-design of navigation and signal control can provide.

Prior work has pursued three main directions to address these shortcomings. Fixed-time optimization methods [5–8] refine signal timing plans using historical or probe data, improving the delay and progression in targeted scenarios, but their reliance on pre-specified demand assumptions makes them brittle under non-stationary or incident-driven traffic. Adaptive and learning-based methods [9–16] apply reinforcement learning or connected-vehicle sensing to adjust phase decisions in real time, yet they still operate at the individual intersection level and do not coordinate with route guidance, leaving the navigation–signal decoupling problem unresolved. Integrated navigation–signal studies [17–21] jointly optimize routing and signal timing to improve network-level progression, but they commonly require significant computational overhead that limits practical scalability. None of these approaches combine a lightweight, congestion-contribution-based navigation service with an enhanced compatible-phase-combination signal controller in a unified, computationally tractable framework that remains effective under moderate-to-heavy CAV traffic.

To address these gaps, we propose CATS, a Context-Aware Traffic Signal control system that tightly co-designs intersection signal control and road navigation for CAVs, as illustrated in Figure 1. With the transportation infrastructure information, vehicle mobility information, and traffic signal state information, CATS integrates two components built on top of existing foundations: Best-Combination CTR (BC-CTR) and the Self-Adaptive Interactive Navigation Tool (SAINT). BC-CTR enhances the original CTR scheme by first identifying the phase with the highest cumulative travel time (CTT) and then searching between its compatible phase combinations to select the group with the greatest combined CTT, thereby making more demand-aware phase-switching decisions. SAINT complements BC-CTR by computing a Congestion Contribution Step Function (CCSF) for each vehicle to quantify how much remaining congestion lies ahead on its route, and uses this to steer newly arriving vehicles toward less-congested paths. Because SAINT incorporates traffic-signal waiting time into its path-cost estimate, it remains consistent with the phase decisions made by BC-CTR, enabling the two components to interact and produce combined improvements in both E2E travel time and network throughput.

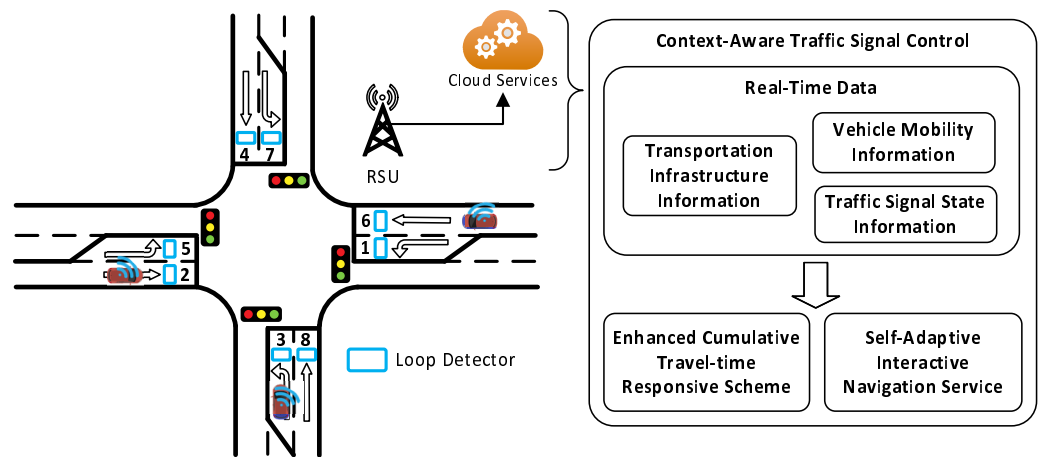


**Figure 1.** Overview of CATS architecture.

In this paper, the term *context-aware* refers to using both local intersection state and network-level route context for control decisions, rather than relying on local demand only. Specifically, CATS uses (i) phase-level and compatible-group CTT at each intersection, (ii) road-segment delay and route-level E2E delay estimated from network traffic observations, (iii) CCSF-based congestion contribution values that indicate downstream congestion remaining along each vehicle route, and (iv) expected incoming demand shaped by SAINT's route guidance updates. Existing adaptive signal methods typically optimize phase switching from local intersection observations, while CATS additionally incorporates this network-level contextual information from navigation-side congestion estimation to better align signal timing with city-scale traffic evolution.

The key technical contributions are summarized as follows:

- We designed BC-CTR, an enhanced actuated signal control scheme that extends the original CTR by first selecting the phase with the highest cumulative travel time (CTT) and then identifying the compatible phase combination with the greatest group CTT. This two-step selection allows the controller to respond more accurately to real-time intersection demand than the single-combination evaluation in the original CTR.
- We integrated BC-CTR with SAINT, a congestion-contribution-based navigation service, into a unified CATS framework. SAINT quantifies the remaining congestion on each vehicle's route and steers incoming vehicles toward less-congested paths, while incorporating traffic-signal waiting time into path costs so that navigation remains consistent with BC-CTR's signal decisions.
- We evaluated CATS's performance through SUMO-based simulations spanning heavy to light traffic and compared it with three baselines. Under moderate-to-heavy traffic, CATS reduces the mean E2E travel time by up to 23.72% and improves the throughput by up to 93.19% over the baselines, demonstrating that the co-design of navigation and signal control produces complementary benefits.

The rest of this paper is organized as follows. Section 2 summarizes and analyzes the existing related work. Section 3 describes the system design of our proposed method, which includes the preliminary schemes. Section 4 shows the performance evaluation of the proposed method. Section 5 discusses the implications of our results and potential limitations. Finally, in Section 6, we conclude this paper, along with discussing potential future work.

## 2. Related Work

In this section, we introduce the related work for optimizing traffic signal control. We surveyed the recent studies on traffic signal control optimization, categorizing them

into three main approaches: fixed-time-oriented optimization, adaptive signal control, and integrated navigation-signal control.

For fixed-time-oriented optimization, recent studies include probe-data-assisted timing design [5], network-level joint signal/trajectory optimization for mixed traffic [6], bee-colony-based plan search for superstreet fixed-time control [7], coordinated offset optimization via flow- and bandwidth-based formulations [8], constrained cycle/split optimization for isolated intersections under environmental and non-motorized constraints [22], vision-assisted multi-intersection timing updates [23], and method-level optimization for urban multi-leg intersections [24]. Their main benefit is improved delay, progression, or emissions under target scenarios, but common limitations remain: strong dependence on scenario-specific demand assumptions; limited robustness under incident-driven nonstationary traffic; and reduced transferability when network geometry, sensing quality, or connected-vehicle penetration changes.

Recent adaptive signal-control studies mainly adopt learning-based methods. Cao et al. [9] applied deep reinforcement learning to optimize phase-switching decisions from real-time intersection states, while Cai and Wei [10] improved the DQN-style training stability for urban adaptive control under varying demand. Kamal et al. [11] combined a digital twin with deep reinforcement learning to reduce the simulation-to-deployment gap during policy development. Mo et al. [12] proposed a decentralized connected-vehicle-based learning framework (CVLight) to improve scalability and local responsiveness. Fu et al. [13] presented an improved D3QN phase-control strategy for isolated intersections to better balance delay and queue evolution. Although these studies report improved delay or throughput, common limitations remain: many evaluations are conducted in simulated or isolated-intersection settings, performance can depend on penetration and quality of connected-vehicle sensing, and policy transferability across cities and mixed traffic compositions is still limited.

Moreover, recent studies have explicitly integrated traffic signal control with navigation and route guidance. Cao et al. [17] used navigation requests to reserve coordinated green-wave opportunities, Menelaou et al. [18] jointly optimized route guidance and regional demand management for real-time network control, Guo et al. [19] proactively coordinated guidance and signal control in divergent networks, Zhang et al. [20] coupled dynamic route guidance with signal timing under accident-induced congestion, and De Souza et al. [21] formulated a joint routing-signal multi-commodity optimization for connected vehicles. These approaches improve progression, throughput, or resilience in targeted scenarios, but common limitations include assumptions on communication reliability and penetration, high computational/coordination overhead at scale, and limited validation under heterogeneous real-world driver compliance.

According to the above analysis, however, most existing systems do not fully leverage the potential of context-aware data from navigation services to optimize traffic signal control. To the best of our knowledge, no prior work combines a primary-phase-first, best-compatible-group signal controller with a congestion-contribution-based navigation mechanism in a single, low-overhead framework. Rule-based logic such as BC-CTR is preferable to learning-based methods for roadside-unit deployment because it requires no training data, has deterministic and bounded response latency, and supports interpretable field calibration, which are properties that are essential for safety-critical infrastructure. In this work, we aim to fill this gap by proposing a Context-Aware Traffic Signal control optimization system that integrates road navigation services for improved traffic management. Table 1 summarizes the main differences between the representative approach categories and CATS. The comparison is based on five key criteria: real-time adaptation, network-wide context, route-signal integration, lightweight online logic, and end-to-end

(E2E) travel time plus throughput evaluation, where the symbol × indicates that the criterion is not met, the symbol ✓ indicates that the criterion is met, as shown in Table 1. CATS is the only approach that meets all five criteria, demonstrating its unique contribution to the field of traffic signal control optimization.

**Table 1.** Comparison of existing approaches and the proposed CATS.

Approach	Real-Time Adaptation	Network-Wide Context	Route-Signal Integration	Lightweight Online Logic	E2E + Throughput Evaluation
Fixed-time-oriented	×	×	×	✓	×
Adaptive signal control	✓	×	×	×	×
Integrated navigation-signal	✓	✓	✓	×	×
Proposed CATS	✓	✓	✓	✓	✓

### 3. System Design

In this section, we first give a brief overview of the original CTR scheme and SAINT system, which are the basis of our proposed system. Then, we introduce the design of our proposed Context-Aware Traffic Signal (CATS) control optimization system, which integrates an enhanced CTR scheme and SAINT system to improve road traveling efficiency.

#### 3.1. Preliminaries

The original CTR scheme and SAINT system are the basis of our proposed system. CTR scheme is an actuated traffic signal control method that adjusts traffic signal timings based on the cumulative travel time (CTT) of vehicles approaching an intersection. The SAINT navigation system provides real-time route guidance to drivers based on current traffic conditions, utilizing a congestion prediction mechanism to suggest optimal routes that minimize travel time and avoid congested areas.

##### 3.1.1. Cumulative Travel-Time Responsive Scheme (CTR)

The Cumulative Travel-Time Responsive (CTR) [4,25] scheme is an actuated traffic signal control method that adjusts traffic signal timings based on the cumulative travel time (CTT) of vehicles approaching an intersection. The CTT is defined as the summation of driving time of all vehicles at current phase (road or lane) of a road segment. As shown in Figure 2, assume that there are multiple phases at an intersection, each phase corresponds to a specific movement direction (e.g., straight, left turn, right turn) for vehicles approaching the intersection from different road segments. We can calculate the CTT for each phase by summing the travel times of all vehicles waiting at that phase. For example, in Figure 2 the Road Segment A has two phases: *Phase<sub>6</sub>* for straight movement and *Phase<sub>1</sub>* for left turn movement. The CTT of *Phase<sub>6</sub>* is calculated by summing the travel times of all vehicles waiting for straight movement, while the CTT of *Phase<sub>1</sub>* is calculated by summing the travel times of all vehicles waiting for left turn movement. Specifically, assume that there are *n* vehicles at phase *i*, and the travel time of vehicle *j* is *t<sub>ij</sub>*; then, the CTT of phase *i* can be calculated as follows:

$$CTT_i = \sum_{j=1}^n t_{ij} \tag{1}$$

Figure 3 illustrates the working principle of the CTR scheme. When starting, the CTR scheme checks the CTT of each phase at an intersection. Then, it selects the phase (i.e., *Phase<sub>h</sub>*) with the highest CTT to compare it with the current phase (i.e., *Phase<sub>c</sub>*). If the CTT of *Phase<sub>h</sub>* is larger than that of *Phase<sub>c</sub>* by a predefined threshold, the traffic signal will switch to green for *Phase<sub>h</sub>*, allowing vehicles to pass through the intersection. Otherwise, the current phase will continue to have the green signal. In either case, based on a timer, the

CTR scheme will periodically check the CTT of each phase to make further decisions. The timer is generally set to a few seconds (e.g., 5 s) to ensure a timely response to changing traffic conditions.

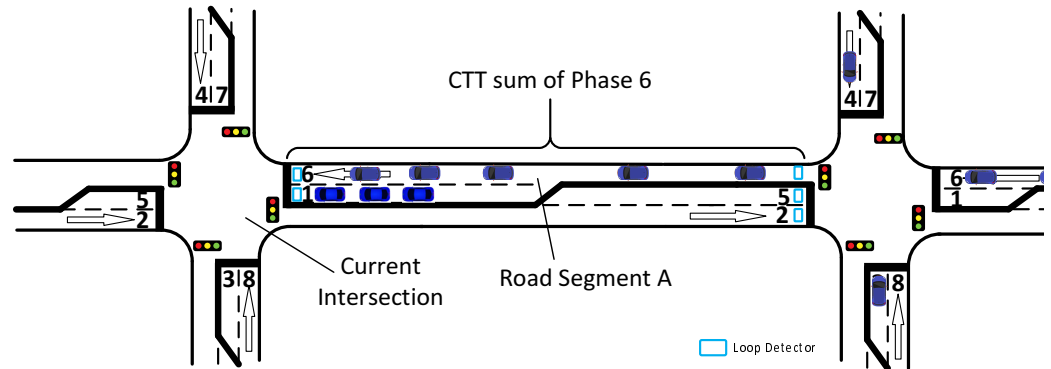


Figure 2. Calculation of cumulative travel time value.

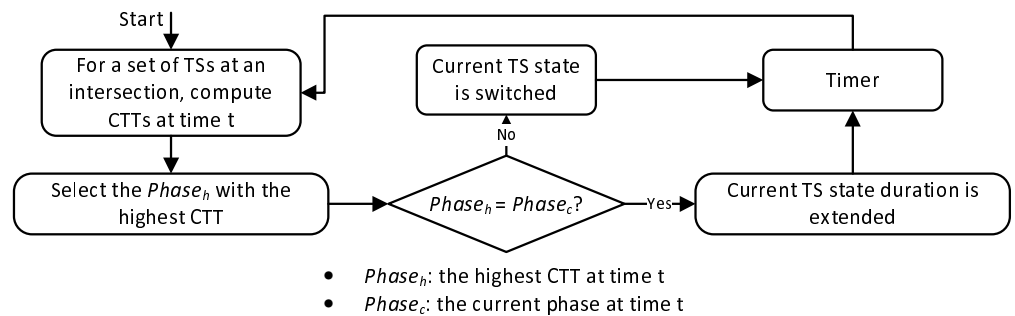


Figure 3. Working principle of CTR scheme.

As shown in Figure 3, by monitoring the CTT, the CTR scheme can dynamically allocate green signal time to phases with higher traffic demand, thereby improving traffic flow and reducing congestion at intersections.

### 3.1.2. Self-Adaptive Interactive Navigation Tool (SAINT)

The self-adaptive interactive navigation tool (SAINT) [26,27] is a road navigation service that provides real-time route guidance to drivers based on current traffic conditions. It utilizes a congestion prediction mechanism to suggest optimal routes that minimize travel time and avoid congested areas.

The congestion prediction mechanism relies on the travel time of each road segment. In practice, the travel time of an individual road segment or an E2E path can be measured using various methods, such as cameras or loop detectors. Assume that during a sampling period  $T$ , the number of vehicles traveling on road segment  $(r_i, r_j)$  is  $n$ , where  $(r_i, r_j)$  denotes an edge connecting vertices  $r_i$  and  $r_j$ . Let  $t_{v_i}$  denote the travel time of vehicle  $v_i$  on this segment. Then, the mean travel delay  $d_{(r_i, r_j)}$  for road segment  $(r_i, r_j)$  is calculated as follows:

$$d_{(r_i, r_j)} = \begin{cases} \frac{\sum_{i=1}^n t_{v_i}}{n} & n > 0, \\ \frac{l_{(r_i, r_j)}}{s_L} + \overline{d_{TL}} & n = 0, \end{cases} \quad (2)$$

where  $l_{(r_i, r_j)}$  denotes the length of road segment  $(r_i, r_j)$ ,  $s_L$  denotes its speed limit, and  $\overline{d_{TL}}$  denotes the average traffic-light waiting time. Equation (2) considers two cases. If vehicles are traveling on the road segment during the sampling period,  $d_{(r_i, r_j)}$  is calculated as the average travel time of those vehicles. If no vehicle travels on the segment during the sampling period,  $d_{(r_i, r_j)}$  is estimated as the travel time based on the segment length and

speed limit, plus the average traffic-light waiting time. Note that  $t_{v_i}$  includes the waiting time at the traffic light at the intersection before the vehicle enters the next road segment.

For a vehicle  $v_i$  whose route  $R_{v_i}$  consists of a sequence of intersections,  $R_{v_i} = \langle r_1, r_2, \dots, r_n \rangle$ , where  $r_k \in V(G)$ , the E2E delay can be expressed as

$$D_n^{v_i} = \sum_{k=1}^{n-1} d_{(r_k, r_{k+1})}, \tag{3}$$

where  $R_{v_i}$  denotes the set of intersections included in the route of vehicle  $v_i$ .

Based on the *road segment delay* and *E2E delay*, each vehicle is associated with a travel delay on each road segment along its route, referred to as the link delay, as well as an E2E delay for the entire route. For a particular vehicle  $v_j$ , the congestion contribution (CC)  $c_i^{v_j}$  is defined as

$$c_i^{v_j} = 1 - \frac{D_i^{v_j}}{D_n^{v_j}}, \tag{4}$$

where  $D_n^{v_j}$  denotes the E2E delay of vehicle  $v_j$  for a travel path with  $n$  vertices, that is, the travel delay from source intersection 1 to destination intersection  $n$ , and  $D_i^{v_j}$  denotes the sub-route delay from source intersection 1 to an intermediate intersection  $i$ :

$$D_i^{v_j} = \begin{cases} \sum_{k=1}^{i-1} d_{(r_k, r_{k+1})} & \text{for } i \geq 2, \\ 0 & \text{for } i = 1, \end{cases} \tag{5}$$

where  $d_{(r_k, r_{k+1})}$  denotes the travel delay of road segment  $(r_k, r_{k+1})$  in the route. Note that  $D_1^{v_j}$  is defined as 0 because it represents the delay at the start of the route, and the corresponding CC value  $c_1^{v_j}$  is 1.

Since  $c_i^{v_j}$  remains invariant on each road segment of a route, we define the Congestion Contribution Step Function (CCSF)  $C_i^{v_j}(x)$  for the sub-route delay  $x$  from the vehicle's starting position to an intermediate position on its trajectory:

$$C_i^{v_j}(x) = c_i^{v_j} \cdot u(x - D_i^{v_j}), \tag{6}$$

where  $u(x - D_i^{v_j})$  is a shifted unit step function defined as

$$u(x - D_i^{v_j}) \triangleq \begin{cases} 1 & x \geq D_i^{v_j} \\ 0 & x < D_i^{v_j} \end{cases} \text{ for } i \in (1, n). \tag{7}$$

As shown in Figure 4, for the vehicle  $v_2$  a set of the CC values  $C_i^{v_2}(D_i)$  is calculated based on the CCSF (6) that decreases CC values of a road segment where the vehicle will travel. The whole road network is updated by the CC values from all vehicles and each road segment has a weight value  $m_{ij}$ . The route of the vehicle virtually affects new joined vehicles in the whole road network. The new joined vehicles are navigated by the less congested path.

In the next section, we introduce the design of our proposed Context-Aware Traffic Signal (CATS) control optimization system, which integrates an enhanced CTR scheme and SAINT system to enhance traffic signal control and navigation services.

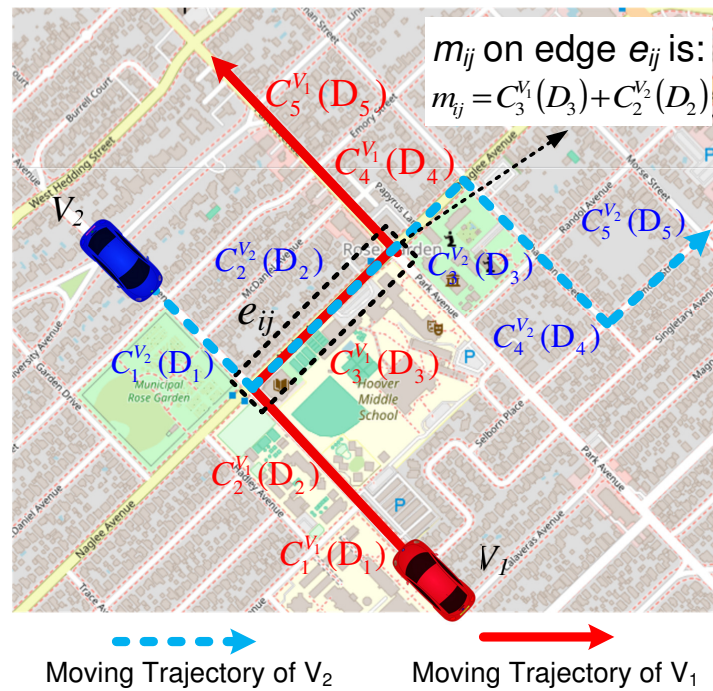


Figure 4. Congestion contribution concept in SAINT.

### 3.2. Context-Aware Traffic Signal (CATS) Control System

In this section, we describe the design of Context-Aware Traffic Signal (CATS) control system. We first introduce the design of the enhanced CTR scheme, which is a key component of CATS. Then, we describe how to integrate the enhanced CTR scheme with SAINT to achieve better performance in terms of traffic flow throughput and travel time.

#### 3.2.1. Enhanced CTR

CTR controls traffic signals of an intersection by monitoring cumulative travel time (CTT) from each incoming road segment. The CTT is defined as the summation of driving time of all vehicles at current phase (lane) of a road segment, as shown in Figure 2. The CTT of a phase at an intersection changes by vehicle traffic. When the CTT of a phase becomes the largest among all CTTs of phases, the traffic signal of this phase shall be switched to a green signal so that vehicles can pass.

As shown in Figure 5, assuming that phase 6 has the largest CTT among all phases, the original CTR will directly select the phase combination of phase 6 (i.e., the option B) to switch to a green signal. In contrast, our proposed enhanced CTR will select the compatible phases of phase 6, and then compare the group CTT of the compatible phases (e.g., phase 2 and phase 1) of phase 6 to make the switching decision. In Figure 5, there could be two options to switch traffic signals. Option B is to select phases 6 and 1, whereas option A is to select phase 6 and 2 since they are compatible. The enhanced CTR will compare the group CTT of the phase combination of phase 6 and phase 2 with the group CTT of the phase combination of phase 6 and phase 1, and select the one with larger group CTT to switch to green signal. In this way, the enhanced CTR better reflects real-time traffic conditions by considering more traffic information from compatible phases, which can lead to better performance in terms of traffic flow and congestion reduction. We call the enhanced CTR the Best-Combination CTR (BC-CTR) since it considers the best combination of phases for the current traffic state.

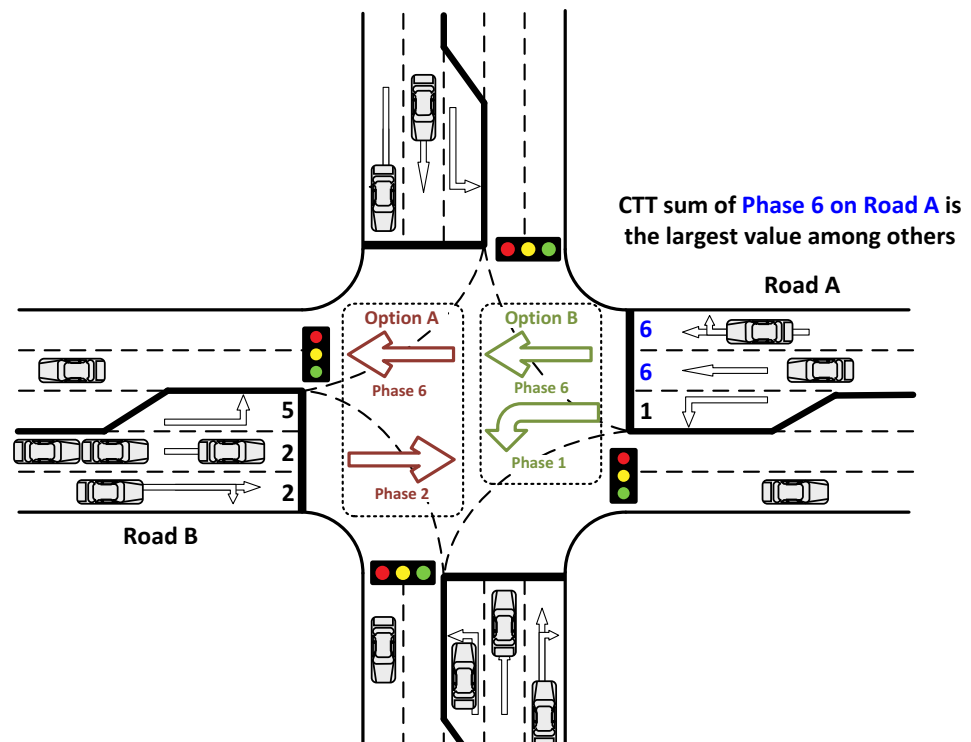


Figure 5. An example of the phase selection scenario.

On top of the original CTR scheme, we formalize BC-CTR as follows. For a signalized intersection, let the phase set be  $\mathcal{P} = \{1, 2, \dots, M\}$ , and let  $CTT_i(k)$  denote the CTT of phase  $i$  at decision epoch  $k$ . We first select the primary phase as

$$h^*(k) = \arg \max_{i \in \mathcal{P}} CTT_i(k). \tag{8}$$

To model movement conflicts (e.g., a protected left turn conflicting with opposite through traffic), we define a binary conflict matrix  $\mathbf{X} = [x_{ij}]$ , where

$$x_{ij} = \begin{cases} 1, & \text{if phases } i \text{ and } j \text{ have a geometric or temporal conflict,} \\ 0, & \text{otherwise.} \end{cases} \tag{9}$$

Using  $\mathbf{X}$ , the set of feasible compatible phase groups containing the primary phase is

$$\mathcal{G}(h^*) = \{g \subseteq \mathcal{P} \mid h^* \in g, x_{ij} = 0 \forall i, j \in g, i \neq j\}. \tag{10}$$

For each candidate group  $g \in \mathcal{G}(h^*)$ , BC-CTR computes the group CTT:

$$CTT_g(k) = \sum_{i \in g} CTT_i(k), \tag{11}$$

and selects

$$g^*(k) = \arg \max_{g \in \mathcal{G}(h^*)} CTT_g(k). \tag{12}$$

Let  $g_c(k)$  denote the currently active compatible group. BC-CTR switches to  $g^*(k)$  only when

$$CTT_{g^*}(k) - CTT_{g_c}(k) > \theta, \tag{13}$$

where  $\theta$  is the same switching threshold concept used in CTR; otherwise, it keeps the current group. Therefore, conflicts are handled explicitly by the constraint  $x_{ij} = 0$ , and only pairwise non-conflicting phase combinations are admissible for green allocation.

In our evaluation,  $\theta$  is set to zero so that any strictly positive group-CTT advantage triggers a switch, matching the maximally responsive setting used in the original CTR field trials [25]. A non-zero  $\theta$  suppresses rapid back-and-forth switching and improves signal stability at the cost of slower demand response; a dedicated sensitivity study of the stability–responsiveness trade-off is planned as future work.

Regarding scalability, for an intersection with  $M$  movements, the compatible-group set  $\mathcal{G}(h^*)$  has at most  $2^{M-1}$  candidate subsets; conflict pruning by  $\mathbf{X}$  reduces this substantially in practice. For the standard four-way intersection ( $M = 8$ ) used in this paper, the search is computationally trivial. For genuinely large or unconventional layouts (e.g.,  $M > 12$ ), a greedy bounded-search strategy for (12) can be applied without modifying the broader CATS framework.

### 3.2.2. Working Process of CATS

The working process of BC-CTR is shown in Figure 6. BC-CTR has a timer to periodically check traffic conditions, e.g., every 5 s. When the timer ends, the CTT of each phase at an intersection will be calculated. Then BC-CTR finds the phase with the largest CTT and searches for its compatible phases. The compatible phases can be classified into two groups: current group (CG) and opposite group (OG). This two-group partition is consistent with the standard two-ring phase structure produced by SUMO’s NETGENERATE for a four-way intersection; the general formulation in (10)–(12) supports an arbitrary number of compatible groups for more complex intersection layouts. For each group, the group CTT is calculated by summing the CTTs of all phases in the group. BC-CTR will compare the CTTs of the two groups and select the group with larger CTT to generate traffic signal states. The generated traffic signal states will be compared with the current traffic signal states to make the switching decision. If the generated traffic signal states are different from the current traffic signal states, the traffic signals will be switched to the generated traffic signal states. Otherwise, the current traffic signal states will be maintained. This process will be repeated periodically to adapt to the changing traffic conditions at the intersection.

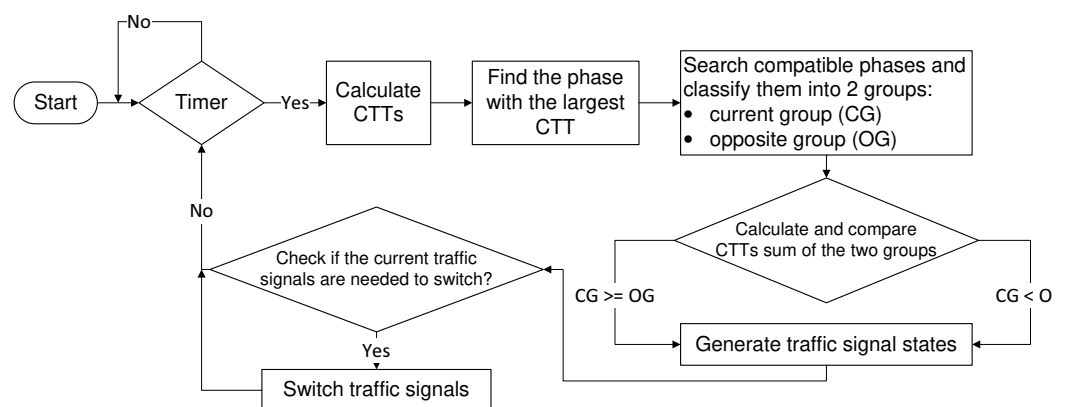


Figure 6. BC-CTR working process.

### 3.2.3. Integration with Road Navigation Services

CATS integrates the proposed BC-CTR and the SAINT system to provide a better driving experience in a traffic-signal rich area. When a vehicle requests route guidance from SAINT, SAINT provides an optimized route based on current traffic conditions and projected future road network conditions. When the vehicle is driving along the suggested

route, BC-CTR will control traffic signals at intersections based on the real-time vehicle traffic status.

Since SAINT considers the waiting time at traffic signals in its route guidance, though the traffic signals are controlled by BC-CTR, SAINT can still provide an optimized route for the vehicle. More specifically, in the integrated CATS setting, we interpret the link cost used by SAINT as the sum of a road-travel component and a signal-delay component:

$$d_{(r_i,r_j)} = d_{(r_i,r_j)}^{road} + \lambda d_{(r_i,r_j)}^{sig} \quad (14)$$

where  $d_{(r_i,r_j)}^{road}$  denotes the running delay on segment  $(r_i, r_j)$ ,  $d_{(r_i,r_j)}^{sig}$  denotes the expected traffic-signal waiting delay before entering the next segment, and  $\lambda$  controls their relative importance in route selection. In the proposed system, we set  $\lambda = 1$  because both terms are measured in seconds and jointly contribute to the end-to-end travel time. Therefore, the integrated path cost is additive and can be written consistently with (2); when observed travel samples are available, the signal-waiting component is already included in the measured link travel time, and when no sample is available, the estimate uses free-flow segment travel time plus average signal delay. This formulation explains how SAINT balances road-segment delay and signal delay while remaining consistent with the signal states generated by BC-CTR. As  $\lambda$  increases above 1, SAINT penalizes any signal-waiting delay more aggressively and steers vehicles away from congested approaches, even at the cost of a longer travel distance; as  $\lambda \rightarrow 0$ , SAINT approaches a travel-distance-only router. Since  $t_{v_i}$  already includes a measured signal-waiting time,  $\lambda = 1$  avoids double-counting while keeping both delay components equally weighted; the sensitivity of system performance to other values of  $\lambda$  is a planned future experiment.

In this way, the navigation and signal control components of CATS are tightly integrated. BC-CTR optimizes signal timings based on real-time traffic conditions, while SAINT provides route guidance that accounts for both road congestion and expected signal delays. This co-design allows CATS to achieve better performance in terms of traffic flow throughput and travel time compared with systems that optimize navigation and signal control separately.

#### 4. Performance Evaluation

We used SUMO (Simulation of Urban MObility) [28] to conduct simulations. The grid road network was generated by the NETGENERATE tool in SUMO. For measuring the road segment travel time, we use TLSE3Detectors tool in SUMO to generate loop detectors. For the loop detectors, instead of using the default detected information (e.g., speed, vehicle count, occupancy) using a pair of loop detectors at a single location of a road segment, using two pairs of detectors located at two ends of a road segment, we modified the original function to calculate the travel time of each vehicle on the road segment so that the mean travel time of the road segment for a given time interval can be calculated. We used the TraCI [28] APIs of SUMO to control all the process of CATS. The simulation setup is shown in Figure 7.

All vehicles in the simulation were treated as CAVs: they complied fully with SAINT route guidance and supplied real-time travel-time data to the infrastructure through the TraCI interface, representing a 100% CAV penetration scenario with instantaneous and lossless Vehicle-to-Infrastructure (V2I) communication. The implications of relaxing this idealized assumption, including partial penetration rates and mixed-traffic scenarios, are discussed in Section 5.

Other simulation environment parameters are in Table 2. For the road networks, we used a grid road network for simulation. In this grid road network, each road segment

had three lanes, with a dedicated lane for left turns. To make the simulation more realistic, we added a 2 s yellow signal time for the transition between green and red signals. This transition time can mitigate aggressive driving behaviors of vehicles inside intersection areas due to sudden traffic light switching. The road network used in the simulation can reflect a real-world traffic-signal rich area (e.g., Manhattan area), where there are many intersections with traffic signals.

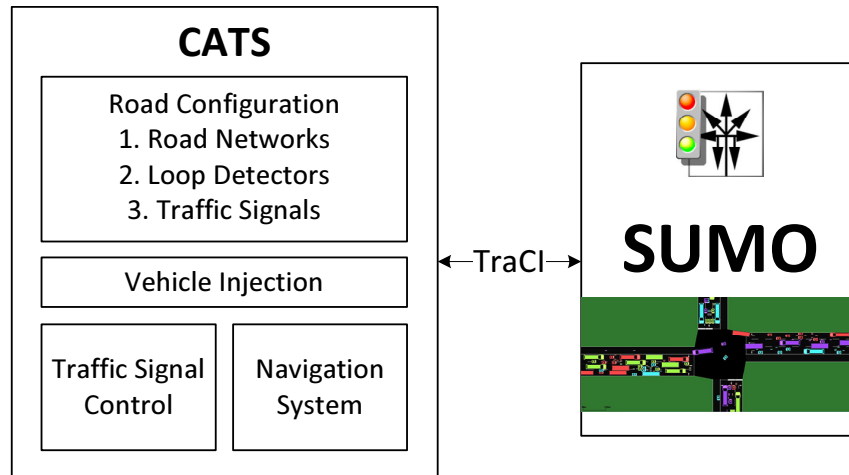


Figure 7. Simulation setup.

Also, in our simulation, the  $X$  in (9) was derived from standard phase-conflict definitions of NETGENERATE in SUMO for the four-way intersection: two phases  $i$  and  $j$  satisfy  $x_{ij} = 1$  if their vehicle trajectories cross geometrically or if they correspond to opposing through-and-protected-left-turn movements that cannot be served simultaneously under SUMO’s standard two-ring actuated phase structure.

Table 2. Simulation setup configuration.

Parameter	Configuration/Value
Road network	A $4 \times 4$ grid road network with 3 lanes per road segment
Road segment length	300 m
Vehicle speed limit	80 km/h
Traffic signal control	BC-CTR, CTR
Vehicle navigation schemes	SAINT, Dijkstra
Vehicle inter-arrival time	5 s, 7 s, 9 s, 11 s, 13 s, 15 s
Performance metrics	Throughput, end-to-end (E2E) travel time
Simulation time	2 h
Number of runs per setting	10

For the performance metrics, we measured both the End-to-End (E2E) and throughput.

- E2E travel time: The total time taken for a vehicle from the fixed locations to travel from its departure point to its destination, including any waiting time at traffic signals.
- Throughput: The total number of vehicles departing from and arriving at the fixed locations that successfully pass through the road network during the simulation period.

To measure the throughput, the vehicle traffic was configured to enter from one side boundary and travel to the opposite side boundary, with random destinations on that boundary, as depicted by the blue arrows at the boundaries in Figure 8, and two pairs of fixed locations were selected for the E2E travel time measurement (i.e., Location Pairs 1 and 2, as shown in Figure 8). To get the E2E travel time, we let 20 vehicles depart from the

two pairs of the fixed locations in the grid road network. For these 20 vehicles, their actual navigated routes may differ depending on traffic conditions. The conducted simulations were open-loop, that is, if a vehicle arrived at its destination, it was removed from the simulation.

The vehicle speed limit was set to 80 km/h, which is a common speed limit in urban areas. The vehicle inter-arrival time is set to 5 s, 7 s, 9 s, 11 s, 13 s, and 15 s to evaluate the performance under different traffic conditions, ranging from heavy traffic (5 s inter-arrival time) to light traffic (15 s inter-arrival time). All the performance metrics were averaged over 10 simulation runs for each setting to ensure the reliability of the results. The results included 90% confidence intervals to show the variability of the performance metrics across different runs.

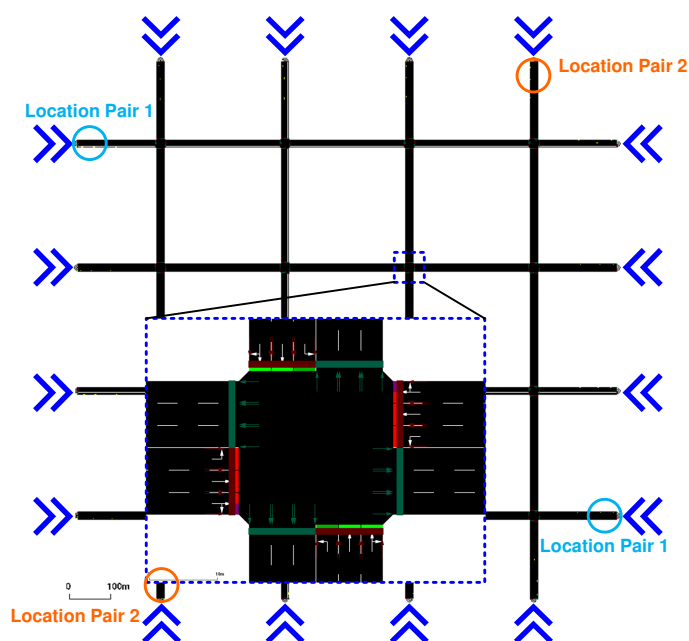


**Figure 8.** Road networks in the simulation environment. The blue arrows at the boundaries indicate the directions of vehicle traffic injection, and the circles indicate the fixed locations for E2E travel time measurement.

To demonstrate the improvement in the proposed CATS method, we compared it with three baseline combinations of two traffic signal control methods (BC-CTR and O-CTR) and two navigation schemes (SAINT and Dijkstra, which were implemented based on Yen's k-shortest path algorithm [29] with graph modeling using the NetworkX library [30] in Python 3.14):

1. **Dijkstra + BC-CTR:** Shortest-time Dijkstra navigation paired with BC-CTR signal control. This isolated the contribution of SAINT by keeping BC-CTR constant.
2. **SAINT + O-CTR:** SAINT congestion-aware navigation paired with the original CTR single-combination signal controller. This isolated the contribution of BC-CTR by keeping SAINT constant.
3. **Dijkstra + O-CTR:** Shortest-time Dijkstra navigation with the original CTR. This was the fully unenhanced baseline.

All four schemes (including CATS) were implemented in SUMO using identical network configurations, vehicle demand profiles, and TraCI control loops; no hyper-parameters beyond  $\theta$  (set to zero for all CTR variants) were tuned differently across the methods, ensuring a fair comparison.

### 4.1. Mean E2E Travel Time

To evaluate the mean end-to-end (E2E) travel time, we varied the vehicle inter-arrival time to generate different traffic states, i.e., from heavy traffic to light traffic, in the simulation. As shown in Figure 9, the mean E2E travel time of CATS (i.e., SAINT with BC-CTR) is the lowest among the four combinations when the vehicle inter-arrival time is large (i.e., 5 s, 7 s, and 9 s). This observation suggests that the proposed CATS method better reflects real-time traffic conditions by considering more traffic information from compatible phases, which can lead to better performance in terms of traffic flow and congestion reduction. However, when the vehicle inter-arrival time increases (i.e., 11 s, 13 s, and 15 s), the mean E2E travel time of CATS is similar to that of SAINT with O-CTR, as well as the other baselines. This observation suggests that when the traffic is light, the performances of CATS and the baselines are similar since the traffic condition is not heavy enough to show the advantage of CATS. In contrast, when the traffic is heavy, CATS better optimizes the traffic signal control by considering more traffic information, leading to a lower E2E travel time.

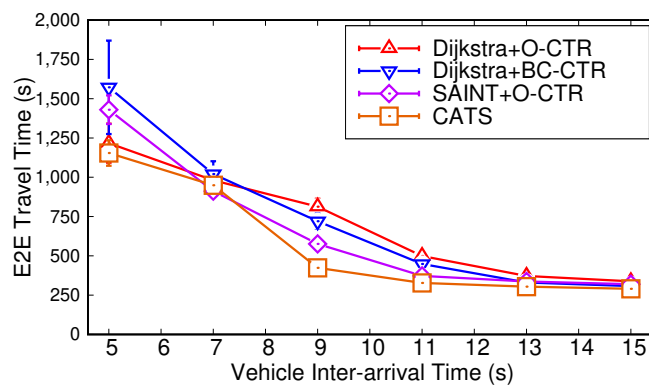


Figure 9. Mean E2E travel time.

Figure 10 shows the cumulative distribution function (CDF) of the mean E2E travel time for CATS and the baselines. From the figure, we can see that the CDF of mean E2E travel time of CATS is mostly higher than that of the other combinations. This observation further confirms that CATS can optimize more effectively the traffic signal control under heavy traffic conditions, leading to lower E2E travel time for vehicles. However, when the vehicle inter-arrival time increases (i.e., 11 s, 13 s, and 15 s), the CDF of the mean E2E travel time of CATS is almost the same as that of the baselines.

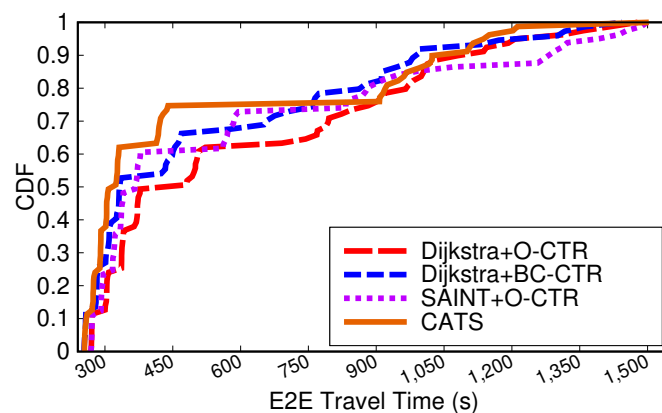


Figure 10. The CDF of mean E2E travel time.

More specifically, CATS achieves mean E2E travel times of 1154.3, 949.0, 423.6, 327.9, 304.3, and 290.2 s at inter-arrival times of 5, 7, 9, 11, 13, and 15 s, respectively. Compared

with SAINT+O-CTR, CATS reduces the mean E2E travel time by 275.6 s (19.27%) at 5 s, 152.5 s (26.47%) at 9 s, 44.3 s (11.91%) at 11 s, 32.7 s (9.71%) at 13 s, and 29.4 s (9.19%) at 15 s. Averaged over the heavier traffic cases of 5, 7, and 9 s, CATS reduces the mean E2E travel time by 13.40% compared with SAINT+O-CTR, 23.72% compared with Dijkstra+BC-CTR, and 16.08% compared with Dijkstra+O-CTR. The largest single reduction is observed at 9 s, where CATS lowers the mean E2E travel time by 296.8 s (41.20%) relative to Dijkstra+BC-CTR and by 389.5 s (47.90%) relative to Dijkstra+O-CTR. These results indicate that the integration of SAINT with BC-CTR is particularly effective in the moderate-to-heavy traffic region.

The CDF figure shows a more nuanced pattern. At the median point, CATS reaches about 324.2 s, which is 42.6 s (11.61%) lower than SAINT+O-CTR and 155.4 s (32.40%) lower than Dijkstra+O-CTR, but only 8.4 s (2.51%) lower than Dijkstra+BC-CTR. At the 90th percentile, CATS reaches about 1100.8 s, which is still 181.9 s (14.18%) lower than SAINT+O-CTR and 36.6 s (3.22%) lower than Dijkstra+O-CTR. However, unlike the throughput figure (Figure 11), the CATS CDF does not strictly dominate all other schemes over the entire range. One unusual observation is that SAINT+O-CTR is slightly better than CATS at 7 s in the mean plot, reducing the travel time by 37.0 s (4.05%) relative to CATS. Another notable point is that the CDF curves cross each other: Dijkstra+BC-CTR has a slightly smaller 25th-percentile value than CATS (284.8 s versus 288.8 s), and CATS has a larger 75th-percentile value than all three baselines (907.0 s versus 833.0 s for SAINT+O-CTR, 761.0 s for Dijkstra+BC-CTR, and 901.7 s for Dijkstra+O-CTR). This suggests that although CATS yields the best average E2E travel time overall, it still exhibits a heavier upper-tail delay in part of the distribution.

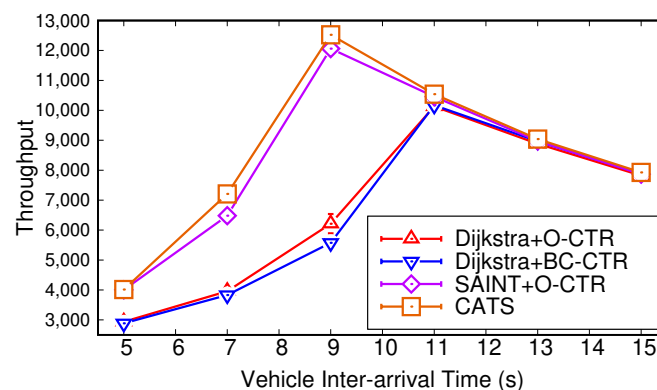


Figure 11. Mean throughput.

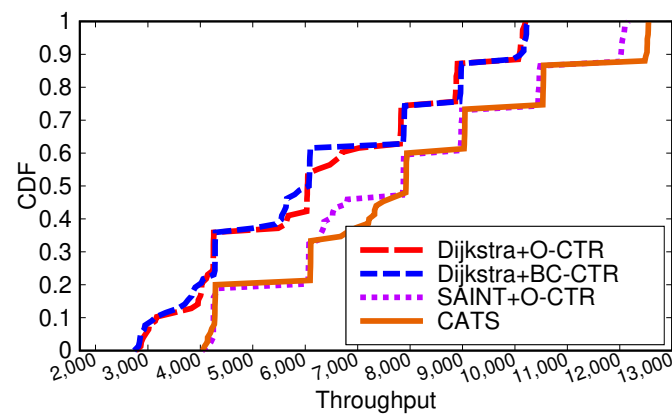
#### 4.2. The Mean Throughput

Figure 11 shows the mean throughput of CATS and the baselines under different vehicle inter-arrival times. From the figure, we can see that the mean throughput of CATS is higher than that of the other combinations when the vehicle inter-arrival time is small (i.e., 5 s, 7 s, and 9 s). This observation suggests that CATS better optimizes the traffic signal control under heavy traffic conditions, leading to higher throughput for vehicles. However, when the vehicle inter-arrival time increases (i.e., 11 s, 13 s, and 15 s), the mean throughput of CATS is similar to that of the baselines. This observation suggests that when traffic is light, the performance of CATS and the baselines is similar because road network conditions are not severe enough to reveal the advantage of CATS.

Figure 12 shows the CDF of mean throughput for CATS and other baselines. From the figure, we can see that the CDF of the mean throughput of CATS is mostly higher than that of the other combinations. This observation further confirms that CATS better optimizes the traffic signal control under heavy traffic conditions, leading to a higher throughput for

vehicles. However, when the vehicle inter-arrival time increases (i.e., 11 s, 13 s, and 15 s), the CDF of the mean throughput of CATS is almost the same as that of the baselines.

More specifically, CATS achieves throughput values of 4015.9, 7207.1, 12524.3, 10539.8, 9040.7, and 7927.1 vehicles at inter-arrival times of 5, 7, 9, 11, 13, and 15 s, respectively. Compared with SAINT+O-CTR, the throughput gains of CATS are 13.5 (0.34%), 727.2 (11.22%), 464.3 (3.85%), 83.0 (0.79%), 64.7 (0.72%), and 56.4 (0.72%) vehicles, respectively. Averaged over the heavier traffic cases of 5, 7, and 9 s, CATS improves the throughput by 5.35% over SAINT+O-CTR, 93.19% over Dijkstra+BC-CTR, and 81.15% over Dijkstra+O-CTR. The largest single gain is observed at 9 s, where CATS outperforms Dijkstra+BC-CTR by 6950 vehicles (124.68%) and Dijkstra+O-CTR by 6311.5 vehicles (101.59%). These results indicate that the navigation component is the dominant factor in throughput improvement, while BC-CTR provides an additional gain on top of SAINT.



**Figure 12.** The CDF of mean throughput.

The CDF figure shows the same trend from a distribution perspective. At the 25th, 50th, 75th, and 90th percentiles, CATS reaches throughput values of about 6100, 7923, 10533, and 12520, respectively. Relative to SAINT+O-CTR, these percentile gains are 38 (0.63%), 52 (0.66%), 90 (0.86%), and 493 (4.10%) vehicles, while the gains over Dijkstra+BC-CTR are much larger, namely, 42.62%, 30.48%, 17.77%, and 23.13%. One unusual observation is that Dijkstra+BC-CTR is slightly worse than Dijkstra+O-CTR under the heavier traffic cases of 5, 7, and 9 s, indicating that BC-CTR alone does not guarantee a throughput gain without the SAINT navigation support. Another notable point is that the throughput is not monotonic with increasing inter-arrival time: all schemes peak around 9–11 s and then decrease at 13 and 15 s because lighter traffic injects fewer vehicles into the road network. In addition, the gain of CATS over SAINT+O-CTR is very small at the most congested 5 s case, but becomes much clearer at 7 and 9 s, suggesting that the benefit of the proposed integration is most visible under moderate-to-heavy traffic rather than at the most saturated operating point.

Overall, the performance evaluation shows that CATS delivers the clearest benefit under moderate-to-heavy traffic. Averaged over the 5, 7, and 9 s inter-arrival settings, CATS reduces the mean E2E travel time by 13.40% relative to SAINT+O-CTR, 23.72% relative to Dijkstra+BC-CTR, and 16.08% relative to Dijkstra+O-CTR, while improving the throughputs by 5.35%, 93.19%, and 81.15% over the same baselines, respectively. The strongest single-case gains appear at 9 s, where CATS lowers the mean E2E travel time by up to 389.5 s (47.90%) and increases the throughput by up to 6950.0 vehicles (124.68%), indicating that the integration of SAINT and BC-CTR produces substantial complementary benefits when congestion is significant.

## 5. Limitations

One limitation of the current CTR design is that it uses phase-based CTT calculation, meaning that CTT is computed for each lane. In practice, however, some vehicles may travel in a lane that does not match their intended turning direction. As a result, their travel times are counted toward the CTT of the lane they currently occupy rather than the movement they actually intend to take, which can reduce the accuracy of the CTT representation.

Another limitation is that the current evaluation is conducted only in a simulated  $4 \times 4$  grid road network with a fixed road-segment length, speed limit, signal-transition setting, and vehicle inter-arrival patterns. Although this setup is useful for controlled comparison, it does not fully capture the diversity of irregular urban networks, heterogeneous intersection layouts, lane drops, incidents, pedestrian phases, bus stops, or communication failures that may affect practical deployment. Relatedly, the simulation assumes that navigation guidance and traffic data are available in a timely and reliable manner, whereas real deployments may experience sensing noise, delayed updates, packet loss, and imperfect compliance by human drivers.

Regarding the 100% CAV penetration assumption, at lower penetration rates, BC-CTR remains functional because its CTT values can be derived from loop-detector measurements that detect all vehicles regardless of connectivity status or traffic monitoring cameras that detect the traveling time of individual vehicles. However, SAINT route guidance would only be received by CAV-equipped vehicles, reducing the load-balancing benefit of congestion-aware routing as the fraction of unguided vehicles increases. In addition, segment-delay estimates become noisier because non-connected vehicles do not report travel-time data. A rigorous sensitivity study of CATS performance across penetration levels (e.g., 25%, 50%, and 75% CAV shares) represents important future work.

Regarding the network-level stability, SAINT's CCSF-based routing distributes newly arriving vehicles across multiple less-congested paths rather than routing all of them onto a single minimum-cost route. This gradual smoothing behavior reduces, but does not eliminate, the risk of Braess's paradox-type secondary congestion or oscillatory rerouting. In highly saturated conditions where most alternative routes are already near capacity, simultaneous rerouting of many vehicles may shift the congestion bottleneck rather than relieving it. Formal analysis of the convergence and stability properties of CCSF-based routing under high load is an open theoretical question and is planned as future work.

The reported results are also limited by the scope of the performance metrics and baselines. We mainly evaluate throughput and E2E travel time, but do not explicitly analyze other important criteria such as queue length, fairness between movements, fuel consumption, emissions, safety-related surrogate metrics, or computational overhead at large scale. In addition, the comparison is restricted to combinations of SAINT, Dijkstra, BC-CTR, and O-CTR. Therefore, the current results show the relative benefit of CATS within this comparison set, but they do not yet establish how CATS would perform against a broader set of modern adaptive or learning-based traffic signal control methods.

Finally, the E2E delay results indicate that the proposed method does not uniformly dominate the alternatives across the entire distribution. In particular, some CDF curves cross each other and SAINT+O-CTR performs slightly better than CATS in one mean-delay setting. This implies that while CATS improves average performance overall, it can still produce unfavorable upper-tail delay behavior in some traffic regimes. A more complete validation therefore requires larger-scale experiments over additional network topologies, longer time horizons, richer demand patterns, and real-world or hardware-in-the-loop data.

## 6. Conclusions

In this paper, we proposed CATS, a Context-Aware Traffic Signal control system that combines BC-CTR with SAINT to jointly optimize phase switching and route guidance for CAVs. BC-CTR improves the original CTR by selecting the highest-CTT phase first and then choosing the compatible phase combination with the largest group CTT, while SAINT steers vehicles away from congested paths using congestion-aware route guidance. SUMO-based simulations show that under moderate-to-heavy traffic (5–9 s inter-arrival time), CATS reduces the mean E2E travel time by up to 23.72% over the baselines, and improves the throughput by up to 93.19% over the same baselines. Future work will focus on movement-aware CTT calculation and integrating a learning-based phase-switching mechanism into BC-CTR to better handle heterogeneous traffic demand and irregular real-world road networks. We also note that the current benchmark does not yet include state-of-the-art reinforcement-learning-based multi-intersection controllers; extending the comparison to such methods is an important direction for establishing the full performance envelope of CATS. Furthermore, the reported results assume full CAV penetration; empirical evaluation under mixed-traffic conditions with partial penetration rates is necessary to characterize the robustness of CATS in near-term deployment scenarios.

**Funding:** This research was funded in part by Basic Science Research Program through the National Research Foundation of Korea (NRF) funded by the Ministry of Education (2022R111A1A01053915); in part by the MSIT (Ministry of Science and ICT), Korea, under the National Program for Excellence in SW (2022-0-01077) supervised by the IITP (Institute of Information & communications Technology Planning & Evaluation) in 2025; in part by the IITP under the Artificial Intelligence Convergence Innovation Human Resources Development grant funded by Korean Government (MSIT) (IITP-2026-RS-2023-00255968); and in part by the Ajou University research fund.

**Data Availability Statement:** The original data in the study are included in the article, and further inquiries can be directed to the corresponding author.

**Acknowledgments:** During the preparation of this study, the author used GitHub Copilot for language editing. The author has reviewed and edited the output and takes full responsibility for the content of this publication. The author would like to thank Jaehoon (Paul) Jeong, Jinho Lee, Saerona Choi, and Byungkyu (Brian) Park for their valuable comments during early phases of this work.

**Conflicts of Interest:** The author declares no conflicts of interest. The funders had no role in the design of the study; in the collection, analysis, or interpretation of data; in the writing of the manuscript; or in the decision to publish the results.

## Abbreviations

The following abbreviations are used in this manuscript:

BC-CTR	Best-Combination Cumulative Travel-Time Responsive
CATS	Context-Aware Traffic Signal control system
CAV	Connected and Automated Vehicle
CC	Congestion contribution
CCSF	Congestion Contribution Step Function
CDF	Cumulative distribution function
CG	Current group
CTR	Cumulative Travel-Time Responsive
CTT	Cumulative travel time
E2E	End-to-end
O-CTR	Original Cumulative Travel-Time Responsive
OG	Opposite group
SAINT	Self-Adaptive Interactive Navigation Tool
SUMO	Simulation of Urban MObility
TraCI	Traffic Control Interface

## References

- Jeong, H.; Shen, Y.; Jeong, J.; Oh, T. A comprehensive survey on vehicular networking for safe and efficient driving in smart transportation: A focus on systems, protocols, and applications. *Veh. Commun.* **2021**, *31*, 100349. <https://doi.org/10.1016/j.vehcom.2021.100349>.
- Rottenstreich, O.; Buchnik, E.; Ferster, S.; Kalvari, T.; Karliner, D.; Litov, O.; Tur, N.; Veikherman, D.; Zagoury, A.; Haddad, J.; et al. Probe-based study of traffic variability for the design of traffic light plans. In *Proceedings of the 2024 16th International Conference on COMmunication Systems & NETworkS (COMSNETS)*; IEEE: New York, NY, USA, 2024; pp. 353–360. <https://doi.org/10.1109/COMSNETS59351.2024.10426953>.
- Mahmud, S.; Day, C.M. Infrastructure-Free Optimization of Traffic Signal Offsets: Identifying Traffic Flow Patterns and Reverse Engineering Signal Timing with Connected Vehicle Data. *Transp. Res. Rec.* **2025**, *2680*, 191–213. <https://doi.org/10.1177/03611981251378136>.
- Lee, J.; Park, B.B.; Yun, I. Cumulative Travel-Time Responsive Real-Time Intersection Control Algorithm in the Connected Vehicle Environment. *J. Transp. Eng.* **2013**, *139*, 1020–1029. [https://doi.org/10.1061/\(ASCE\)TE.1943-5436.0000587](https://doi.org/10.1061/(ASCE)TE.1943-5436.0000587).
- Li, Y.; Peng, L. Elevating adaptive traffic signal control in semi-autonomous traffic dynamics by using connected and automated vehicles as probes. *IET Intell. Transp. Syst.* **2024**, *18*, 1016–1030. <https://doi.org/10.1049/itr2.12483>.
- Niroumand, R.; Kafashan, F.; Hajibabai, L.; Hajbabaie, A. Real-time network-level traffic signal and trajectory optimization with connected automated and human-driven vehicles. *Comput.-Aided Civ. Infrastruct. Eng.* **2025**, *40*, 5891–5907. <https://doi.org/10.1111/mice.70139>.
- Jovanović, A.; Teodorović, D. Fixed-Time Traffic Control at Superstreet Intersections by Bee Colony Optimization. *Transp. Res. Rec. J. Transp. Res. Board* **2021**, *2676*, 228–241. <https://doi.org/10.1177/03611981211058104>.
- Shams, A.; Mahmud, S.; Day, C.M. Comparison of Flow- and Bandwidth-Based Methods of Traffic Signal Offset Optimization. *J. Transp. Eng. Part A Syst.* **2023**, *040230331*. <https://doi.org/10.1061/JTEPBS.TEENG-7404>.
- Cao, K.; Wang, L.; Zhang, S.; Duan, L.; Jiang, G.; Sfarra, S.; Zhang, H.; Jung, H. Optimization Control of Adaptive Traffic Signal with Deep Reinforcement Learning. *Electronics* **2024**, *13*, 198. <https://doi.org/10.3390/electronics13010198>.
- Cai, C.; Wei, M. Adaptive urban traffic signal control based on enhanced deep reinforcement learning. *Sci. Rep.* **2024**, *14*, 14116. <https://doi.org/10.1038/s41598-024-64885-w>.
- Kamal, H.; Yáñez, W.; Hassan, S.; Sobhy, D. Digital-Twin-Based Deep Reinforcement Learning Approach for Adaptive Traffic Signal Control. *IEEE Internet Things J.* **2024**, *11*, 21946–21953. <https://doi.org/10.1109/JIOT.2024.3377600>.
- Mo, Z.; Li, W.; Fu, Y.; Ruan, K.; Di, X. CVLight: Decentralized learning for adaptive traffic signal control with connected vehicles. *Transp. Res. Part C Emerg. Technol.* **2022**, *141*, 103728. <https://doi.org/10.1016/j.trc.2022.103728>.
- Fu, Z.; Zhang, J.; Tao, F.; Ji, B. Traffic signal phase control at urban isolated intersections: An adaptive strategy utilizing the improved D3QN algorithm. *Meas. Sci. Technol.* **2024**, *36*, 016203. <https://doi.org/10.1088/1361-6501/ad8212>.
- Fan, S.; Lu, K.; Wang, Y.; Tian, X. Action Masking-Based Proximal Policy Optimization with the Dual-Ring Phase Structure for Adaptive Traffic Signal Control. *IEEE Trans. Intell. Transp. Syst.* **2025**, *26*, 2422–2433. <https://doi.org/10.1109/TITS.2024.3510379>.
- Tan, X.; Zhou, Y.; Jiao, X. Traffic Signal Control Based on Deep Reinforcement Learning Using State Fusion and Trend Reward. *Eng. Appl. Artif. Intell.* **2025**, *159*, 111701. <https://doi.org/10.1016/j.engappai.2025.111701>.
- Michailidis, P.; Michailidis, I.; Lazaridis, C.R.; Kosmatopoulos, E. Traffic Signal Control via Reinforcement Learning: A Review on Applications and Innovations. *Infrastructures* **2025**, *10*, 114. <https://doi.org/10.3390/infrastructures10050114>.

17. Cao, M.; Li, V.O.K.; Shuai, Q. Book Your Green Wave: Exploiting Navigation Information for Intelligent Traffic Signal Control. *IEEE Trans. Veh. Technol.* **2022**, *71*, 8225–8236. <https://doi.org/10.1109/TVT.2022.3176620>.
18. Menelaou, C.; Timotheou, S.; Kolios, P.; Panayiotou, C.G. Joint Route Guidance and Demand Management for Real-Time Control of Multi-Regional Traffic Networks. *IEEE Trans. Intell. Transp. Syst.* **2022**, *23*, 8302–8315. <https://doi.org/10.1109/TITS.2021.3077870>.
19. Guo, Y.; Zhang, K.; Chen, X.; Li, M. Proactive Coordination of Traffic Guidance and Signal Control for a Divergent Network. *Mathematics* **2023**, *11*, 4262. <https://doi.org/10.3390/math11204262>.
20. Zhang, H.; Guo, S.; Long, X.; Hao, Y. Combined Dynamic Route Guidance and Signal Timing Optimization for Urban Traffic Congestion Caused by Accidents. *J. Adv. Transp.* **2023**, *2023*, 1–16. <https://doi.org/10.1155/2023/5858614>.
21. De Souza, F.; Carlson, R.C.; Muller, E.R.; Ampountolas, K. Multi-Commodity Traffic Signal Control and Routing With Connected Vehicles. *IEEE Trans. Intell. Transp. Syst.* **2022**, *23*, 4111–4121. <https://doi.org/10.1109/TITS.2020.3041436>.
22. Tran, Q.H.; Do, V.M.; Dinh, T.H. Traffic signal timing optimization for isolated urban intersections considering environmental problems and non-motorized vehicles by using constrained optimization solutions. *Innov. Infrastruct. Solut.* **2022**, *7*, 299. <https://doi.org/10.1007/s41062-022-00895-9>.
23. Zhou, S.; Ng, S.T.; Yang, Y.; Xu, J.F. Integrating computer vision and traffic modeling for near-real-time signal timing optimization of multiple intersections. *Sustain. Cities Soc.* **2021**, *68*, 102775. <https://doi.org/10.1016/j.scs.2021.102775>.
24. Ma, Q.; Zeng, H.; Wang, Q.; Ullah, S. Traffic Optimization Methods of Urban Multi-leg Intersections. *Int. J. Intell. Transp. Syst. Res.* **2021**, *19*, 417–428. <https://doi.org/10.1007/s13177-020-00245-y>.
25. Choi, S.; Park, B.B.; Lee, J.; Lee, H.; Son, S.H. Field implementation feasibility study of cumulative travel-time responsive (CTR) traffic signal control algorithm. *J. Adv. Transp.* **2016**, *50*, 2226–2238. <https://doi.org/10.1002/atr.1456>.
26. Jeong, J.; Jeong, H.; Lee, E.; Oh, T.; Du, D.H.C. SAINT: Self-Adaptive Interactive Navigation Tool for Cloud-Based Vehicular Traffic Optimization. *IEEE Trans. Veh. Technol.* **2016**, *65*, 4053–4067. <https://doi.org/10.1109/TVT.2015.2476958>.
27. Shen, Y.; Lee, J.; Jeong, H.; Jeong, J.; Lee, E.; Du, D.H.C. SAINT+: Self-Adaptive Interactive Navigation Tool+ for Emergency Service Delivery Optimization. *IEEE Trans. Intell. Transp. Syst.* **2018**, *19*, 1038–1053. <https://doi.org/10.1109/TITS.2017.2710881>.
28. Lopez, P.A.; Behrisch, M.; Bieker-Walz, L.; Erdmann, J.; Flötteröd, Y.P.; Hilbrich, R.; Lücken, L.; Rummel, J.; Wagner, P.; Wiessner, E. Microscopic Traffic Simulation using SUMO. In Proceedings of the 2018 21st International Conference on Intelligent Transportation Systems (ITSC), Maui, HI, USA, 4–7 November 2018; pp. 2575–2582. <https://doi.org/10.1109/ITSC.2018.8569938>.
29. Yen, J.Y. Finding the K Shortest Loopless Paths in a Network. *Manag. Sci.* **1971**, *17*, 712–716. <https://doi.org/10.1287/mnsc.17.11.712>.
30. Hagberg, A.; Swart, P.J.; Schult, D.A. *Exploring Network Structure, Dynamics, and Function Using NetworkX*; Los Alamos National Laboratory (LANL): Los Alamos, NM, USA, 2008.

**Disclaimer/Publisher’s Note:** The statements, opinions and data contained in all publications are solely those of the individual author(s) and contributor(s) and not of MDPI and/or the editor(s). MDPI and/or the editor(s) disclaim responsibility for any injury to people or property resulting from any ideas, methods, instructions or products referred to in the content.